International Journal of Technology 15(5) 1331-1348 (2024)
Received May 2024 / Revised July 2024 / Accepted August 2024

International Journal of Technology

http://ijtech.eng.ui.ac.id

Investigating the Influence of Dynamic Interaction Between Primary and Secondary Structures on Elastic Floor Response Spectra During Near- and Far-Field Earthquakes: A Comparative Analysis with EC8 Formulation

Madhavi Latha Annamdasu[1], N. Lingeshwaran[1], Surya Prakash Challagulla[2*], Omar Shabbir Ahmed[3], Musa Adamu[3]

[1]Department of Civil Engineering, Koneru Lakshmaiah Education Foundation (Deemed to be University), Vaddeswaram, Guntur (Dt.), Andhra Pradesh, 522302, India
[2]Thornton Tomasetti, M Agile, Baner Pune, Maharashtra-411045, India
[3]Engineering Management Department, College of Engineering, Prince Sultan University, 11586 Riyadh Saudi Arabia

Abstract. Analyzing secondary structures (SSs) during earthquakes is vital due to their vulnerability and potential impact on building functionality and occupant safety. Understanding the seismic performance of SSs requires analyzing the Floor Response Spectra (FRS). This research investigates how the dynamic interaction between the primary structure (PS) and SSs affects the FRS under near-field (NF) and far-field (FF) earthquake conditions. Both the elastic PS and SS are modeled as single-degree-of-freedom (SDOF) systems. The governing equations of motion of the PS and SS are derived and numerically solved using the RK4 method. The study examines the influence of the PS vibration period ($\boldsymbol{T_p}$), tuning ratio ($\boldsymbol{T_r}$), mass ratio ($\boldsymbol{\mu}$), and SS damping ratio ($\boldsymbol{\xi_s}$) on FRS. Twenty horizontal ground motion excitations were selected for the study. Time-history analysis results indicate that the dynamic interaction is negligible at a lower mass ratio ($\boldsymbol{\mu = 0.001}$). For $\boldsymbol{\mu}$ values of 0.01, 0.1, and 0.5, the peak acceleration response of the SS under near-field (NF) excitation decreased by 15.7%, 68.3%, and 79.1%, respectively, and by 15.2%, 68.9%, and 78.8% under far-field (FF) excitation, compared to the uncoupled case. The spectral acceleration response of the SS is significantly influenced by dynamic interaction within $\boldsymbol{0.8 \leq T_r \leq 1.2}$. For $\boldsymbol{T_r < 0.5}$ and $\boldsymbol{T_r > 2}$, dynamic interaction has no effect on FRS across all considered $\boldsymbol{\xi_s}$ and $\boldsymbol{\mu}$ values. Parametric analysis showed that NF earthquakes induce larger FRS peaks compared to FF events. In conclusion, a comparison between simulated FRS and those predicted by Eurocode 8 shows discrepancies, with the code-based formulation often either underestimating or overestimating the FRS magnitude.

Keywords: Dynamic interaction; Far-field earthquakes; Floor response spectra; Near-field earthquakes; Non-structural component

1. Introduction

Certain building components are unable to bear loads and are classified as secondary structures (SSs). The ground motion of an earthquake can be intensified by a structure, resulting in floor accelerations exceeding those of the ground. If secondary structures (SSs) post-earthquake is crucial for maintaining emergency services and public safety and

*Corresponding author's email: cprakash@thorntontomasetti.com, Tel.: +91- 77 0 22 68 69 7
doi: 10.14716/ijtech.v15i5.7084

mitigating financial losses. Despite their designation, secondary structures play a significant role and can sometimes exceed the primary structure (PS) in cost (Murty *et al.*, 2012; Taghavi and Miranda, 2004). Recent decades have highlighted the vulnerability of secondary structures to earthquakes (Faisal *et al.,* 2023; Challagulla, Parimi and Noroozinejad Farsangi, 2022; Kamble *et al.,* 2022; Partono *et al.,* 2022; Kamble, Bharti and Shrimali, 2021; Wang, Shang and Li, 2021; Challagulla, Parimi, and Anmala, 2020; Challagulla, Parimi and Thiruvikraman, 2020; Sullivan, 2020; Filiatrault *et al.,* 2018). For instance, during the 1994 Northridge earthquake in Los Angeles, several major hospitals had to evacuate due to failures in critical secondary systems (Villaverde, 2009). Considering the critical need to protect SSs during earthquakes, additional research is essential to develop dependable design standards based on performance.

Extensive research has been conducted over the years to understand the behavior of secondary structures (SSs) during earthquakes, aiming to protect public safety and mitigate financial losses from resulting damage. The floor response spectrum (FRS) method is a widely used technique for assessing earthquake forces on secondary structures. It is common practice to utilise the FRS technique to determine the input force of a SS (Bhavani and Challagulla, 2023; Challagulla *et al.,* 2023a; 2023b; Pesaralanka *et al.,* 2023; Vyshnavi *et al.,* 2023; Landge and Ingle, 2021; Pramono *et al.,* 2020; Berto *et al.,* 2020; Surana, Singh and Lang, 2018a). Engineers frequently employ this technique in the design of secondary structures. A key assumption of this method is that the secondary structure does not interact with the primary structure, meaning its presence has no influence on the dynamic response of the primary system, and vice versa.

In cases where the secondary structure (SS) carries significant weight, the assumption of independent behavior between the primary structure (PS) and SS may not hold. This interdependence necessitates a comprehensive consideration of the entire structural system to accurately assess seismic performance. As highlighted by (Annamdasu *et al.,* 2024; Salman, Tran and Kim, 2020; Lim and Chouw, 2018; Kelly and Sackman, 1978), the dynamic interaction between the PS and SS can substantially influence the overall response of the structure during seismic events. Neglecting this interaction typically leads to an overestimation of SS demands, resulting in overly conservative designs that may not be cost-effective or efficient. Smith-Pardo *et al.* (2015) emphasize that this overestimation can lead to unnecessary material use and increased construction costs without a corresponding increase in safety or performance. Consequently, understanding and incorporating the dynamic interaction between PS and SS is crucial for accurate seismic performance evaluation and optimized structural design. Research into the seismic performance of secondary structures should, therefore, take into account their interaction with the primary structure. This approach ensures a more realistic and holistic assessment of structural behavior under seismic loads, leading to safe and economical designs. By integrating this dynamic interaction into the analysis, engineers can better predict the actual demands on both primary and secondary structures, leading to more effective mitigation strategies and improved overall structural resilience during earthquakes. The authors have performed numerical analysis to investigate the behavior of the Floor Response Spectrum (FRS). The primary aim of this research is to thoroughly investigate and understand the seismic performance of secondary structures considering their dynamic interaction with primary structures.

Several studies have explored the dynamic properties and interaction effects of integrated systems with a combined oscillator-structure model (Singh and Suarez, 1987; Suarez and Singh, 1987; Igusa and Der Kiureghian, 1985; Sackman and Kelly, 1979; Kelly and Sackman, 1978). However, prior studies have neglected to consider the effect of dynamic characteristics of both primary and secondary structures on the seismic response of secondary structures. While earlier research has explored the seismic response of primary and secondary structures under typical ground motions, there is a gap in understanding the seismic performance of secondary structures under near and far field earthquake excitations. Near-field and far-field ground motions significantly impact structural responses differently than typical ground motions. Near-field ground motions often induce higher acceleration peaks and demand on structures due to their proximity to the fault, causing rapid energy release. In contrast, far-field motions, originating further from the fault, generally produce lower-frequency content and extended shaking duration, leading to different dynamic responses in structures (Mehta and Bhandari, 2023; Lin, 2022; Salimbahrami and Gholhaki, 2022; Zamanian, Kheyroddin and Mortezaei, 2022; Akbari, Rozbahani and Isari, 2021). Therefore, further investigation is warranted in this regard. This study aims to evaluate how near and far field earthquake events affect floor spectral accelerations. This study uses the dynamic interaction between an elastic PS and SS to examine how the SS performs seismically. To evaluate how secondary structures respond to seismic activity, the floor response spectra (FRS) incorporating dynamic interaction between the primary structure (PS) and secondary structure (SS) are analyzed. The study analyses the effects of various factors on the FRS, including the mass ratio, the time period of the PS, and the secondary structure's damping ratio. Finally, comparisons are drawn between the floor response spectra obtained from this study and those derived from existing code-based formulations.

The structure of the paper is as follows: Section 2 provides a brief summary of the modeling of coupled and uncoupled systems. Section 3 addresses the selection of ground motions, along with other relevant details for this study. Section 4 discusses the study results, with a focus on floor response spectra. Finally, Section 5 offers brief concluding remarks.

2. Modelling and Analysis

This study uses a single-degree-of-freedom (SDOF) system for elastic PS and SS. Coupled analysis accounts for the dynamic interaction between the PS and SS, whereas uncoupled analysis neglects this relationship. Figure 1 illustrates the PS connected to an acceleration-sensitive SS. It is assumed in this study that the primary structure's damping ratio (ξ_p) is 5%.

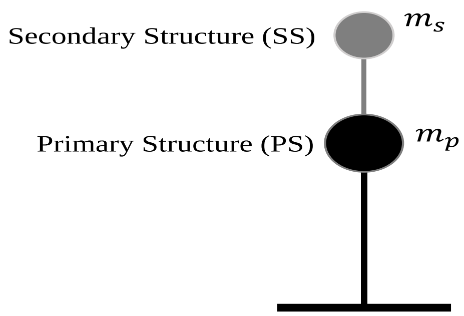

Figure 1 Secondary structure attached to a Primary structure

2.1. Uncoupled Analysis

This analysis method ignores the PS and SS dynamic interaction (see Figure 1). Equation 1 may be used to determine how the PS will respond dynamically to a given earthquake loading.

$$m_p\ddot{x}_p + c_p\dot{x}_p + k_p x_p = -m_p\ddot{x}_g \tag{1}$$

where m_p, c_p, and k_p are the mass, damping, and stiffness of the primary structure: $c_p = 2m_p\xi_p\omega_p$; ω_p is the given primary structure's frequency; x_p, $\dot{x}_p$, and $\ddot{x}_p$ are the relative displacement, velocity, and acceleration of the primary structure with reference to the ground; $\ddot{x}_g$ is the acceleration of the ground motion; $\ddot{x}_p + \ddot{x}_g$ is the primary structure's absolute acceleration response. Equation 2 may be used to compute the SS response, which is then used to assess the SS.

$$m_s\ddot{x}_s + c_s\dot{x}_s + k_s x_s = -m_p(\ddot{x}_p + \ddot{x}_g) \tag{2}$$

where k_s, c_s, and m_s, are the stiffness, damping, and mass of the secondary structure: $c_s = 2m_s\xi_s\omega_s$; ξ_s, and ω_s are the damping ratio and frequency of the SS; x_s, $\dot{x}_s$, and $\ddot{x}_s$ are the relative displacement, velocity, and acceleration of the SS, respectively. Figure 2 shows how to generate the floor response spectrum.

2.2. *Coupled Analysis*

This method studies the dynamic relationship between the structures. The PS and SS's response to a certain dynamic loading can be calculated using Equations 3 and 4, respectively.

$$m_p\ddot{x}_p + c_p\dot{x}_p - c_s\dot{x}_s + k_p x_p - k_s x_s = -m_p\ddot{x}_g \tag{3}$$

$$m_s\ddot{x}_s + c_s\dot{x}_s + k_s x_s = -m_s(\ddot{x}_p + \ddot{x}_g) \tag{4}$$

The matrix version of Equations 3 & 4 is as follows:

$$\begin{bmatrix} m_p & 0 \\ 0 & m_s \end{bmatrix}\begin{Bmatrix} \ddot{x}_p \\ \ddot{x}_s \end{Bmatrix} + \begin{bmatrix} c_p & -c_s \\ 0 & c_s \end{bmatrix}\begin{Bmatrix} \dot{x}_p \\ \dot{x}_s \end{Bmatrix} + \begin{bmatrix} k_p & -k_s \\ 0 & k_s \end{bmatrix}\begin{Bmatrix} u_p \\ u_s \end{Bmatrix} = -\begin{Bmatrix} m_p\ddot{x}_g \\ m_s(\ddot{x}_p + \ddot{x}_g) \end{Bmatrix} \tag{5}$$

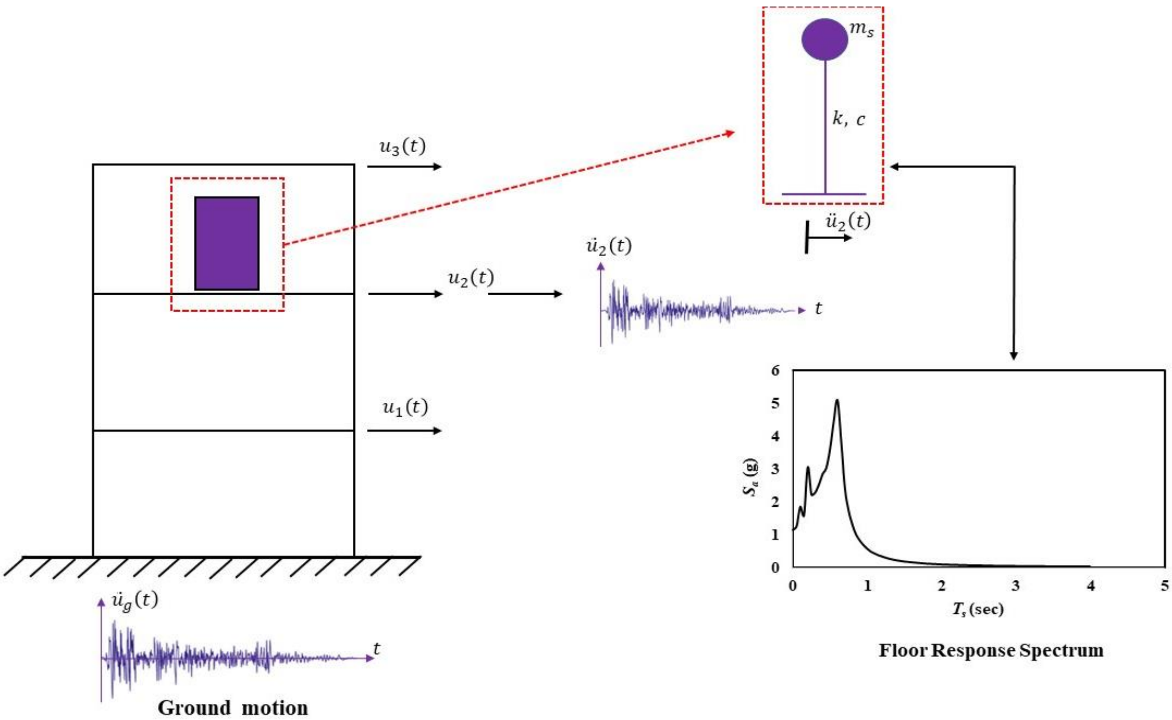

Figure 2 The process of creating floor response spectrum using uncoupled analysis

2.3. *Fourth-Order Runge-Kutta Method for Solving Differential Equations*

In order to solve ordinary differential equations (ODEs) and especially address the dynamic behavior described by the second-order differential equations given in Equations 1– 4, we utilize the Fourth-Order Runge-Kutta (RK4) technique as a numerical tool in this work. The RK4 approach makes it easier to derive dynamic solutions that are necessary to understand how the system reacts to external influences (Challagulla *et al.*, 2023b; Challagulla, Parimi and Thiruvikraman, 2020; Reyes *et al.*, 2020; 2016; Smith-Pardo *et al.*, 2015). This numerical method approximates solutions to ODEs by utilizing known initial conditions. By breaking the problem into smaller segments, the method calculates slopes at various points within each step. The approximation is progressively refined until the desired endpoint is reached by updating the solution at the end of each step. Smaller step sizes lead to greater accuracy, and the precision can be adjusted by modifying the step size (Yaakub and Evans, 1999). The RK4 approach is utilized extensively in several scientific and engineering fields to solve ODEs in situations when precise analytical solutions are not available. This paper presents the steps involved in solving the second-order differential equation given in Equation 1. This is how a first-order system that is equal to the ordinary differential equation in Equation 1 might be redefined Equation 6:

$$\dot{x}_p(t) = v_p(t) \tag{6}$$

$$\dot{v}_p(t) = -\frac{c_p}{m_p} v_p(t) - \frac{k_p}{m_p} x_p(t) - \ddot{x}_g(t) \tag{7}$$

Assuming:

$$X = \begin{pmatrix} x_p(t) \\ v_p(t) \end{pmatrix} \tag{8}$$

$$f\,(t) = \begin{pmatrix} v_p(t) \\ -\frac{c_p}{m_p} v_p(t) - \frac{k_p}{m_p} x_p(t) - \ddot{x}_g(t) \end{pmatrix} \tag{9}$$

The system of autonomous first-order ordinary differential equations (Equations 7 and 7) that follows is produced by combining Equations 8 and 9 with the initial condition $X\,(0) = 0$.

$$\frac{dX}{dt} = f(t), \quad X\,(0) = X_0 \tag{10}$$

The numerical solution of Equation 10 was achieved by the development of a MATLAB code that employs the explicit RK4 technique. Other ODEs, such as Equations 2 – 4, can be solved using the same method described above.

3. Selection and Scaling of Ground Motions

In the context of seismic response assessment, realistic responses are generated by utilizing actual ground-motion records, readily accessible from the Pacific Earthquake Engineering Research Centre (PEER) NGA-West2 Database. Therefore, for the current research, we have incorporated 20 horizontal ground motion excitations, as specified by ASCE 7-16 (ASCE, 2016) tailored for hard soil conditions with a shear wave velocity (V_{s30}) greater than 350 m/sec. Additionally, for this study, we have chosen to employ a set of ground-motion records recommended in FEMA P695 (FEMA, 2009). These records will be used to carry out both linear and nonlinear dynamic analyses on the building structures under consideration, as detailed in Table 1. According to the classification in FEMA P695, the far-field record set comprises ground motions originating from sites situated at a distance equal to or greater than 10 km from the fault rupture. In contrast, the near-field record set includes ground motions recorded at sites located within a distance of less than 10 km from the fault rupture, as determined by the Joyner-Boore distance (R_{jb}). The ground-motion records under consideration were obtained from sites with rock soil conditions, specifically falling within NEHRP site classes B and C. These records are associated with moment magnitudes (M_w) ranging from 6.69 to 7.62, with an average magnitude of 7.05. Among the selected records, the closest distances to the fault rupture, calculated as the average Joyner-Boore distance, span from 0 to 26 km, with an average distance of 8.11 km. The epicentral distances (R_{epi}) for this chosen set of ground motions vary between 4.5 and 86 km, with an average distance of 33.4 km. The peak ground acceleration (PGA) values of these selected records range from 0.22 to 1.49 g, and their average PGA is 0.494 g.. For more comprehensive information regarding these ground motions, further details can be found in FEMA P695. To achieve compatibility with the target response spectrum, which is the Zone V elastic design spectrum of IS 1893 (Part 1): 2016 (Indian Standard, 2016), the chosen ground motion records were subjected to scaling. The process employed for this purpose involved the utilization of a time-domain spectral matching approach to generate earthquake excitations that align with the desired spectrum. The target spectrum, according to IS 1893:2016 (Indian Standard, 2016), is shown in Figure 3, which is linked to 5% damping, along with the mean spectra of ground excitations. In accordance with ASCE 7-16 standards, the mean spectra must not fall below 90% of the target spectrum across the entire period range. It is evident from the figure that the mean spectra comfortably exceed this 90% threshold.

Table 1 Details of near-field and far-field records

S. No	RSN	Earthquake Name	Year	Station Name	M_w	R_{jb} (km)	PGA (g)	R_{epi} (km)
Near field records								
1	802	Loma Prieta	1989	Saratoga - Aloha	6.93	7.58	0.514	27.2
2	821	Erzican_ Turkey	1992	Erzincan	6.69	0	0.386	9
3	828	Cape Mendocino	1992	Petrolia	7.01	0	0.597	4.5
4	1086	Northridge-01	1994	Sylmar - Olive	6.69	1.74	0.604	16.8
5	1165	Kocaeli_ Turkey	1999	Izmit	7.51	3.62	0.165	5.3
6	825	Cape Mendocino	1992	Cape Mendocino	7.01	0	1.49	33.98
7	1004	Northridge-01	1994	LA - Sepulveda	6.69	0	0.752	44.49
Far-field records								
1	953	Northridge	1994	Beverly Hills-Mulhol	6.7	9.4	0.52	13.3
2	1787	Hector Mine	1999	Hector	7.1	10.4	0.34	26.5
3	1111	Kobe, Japan	1995	Nishi-Akashi	6.9	7.1	0.51	8.7
4	1148	Kocaeli, Turkey	1999	Arcelik	7.5	10.6	0.22	53.7
5	900	Landers	1992	Yermo Fire Station	7.3	23.6	0.24	86
6	1633	Manjil, Iran	1990	Abbar	7.4	12.6	0.51	40.4
7	125	Friuli, Italy	1976	Tolmezzo	6.5	15	0.35	20.2

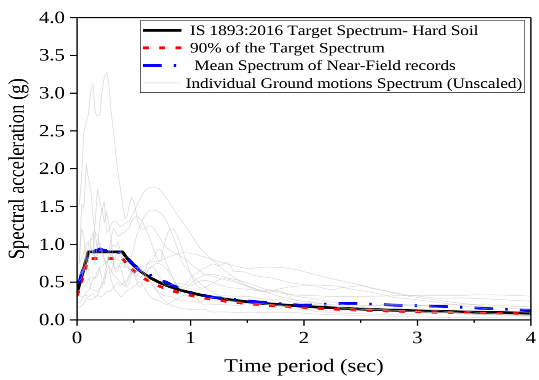

(a)

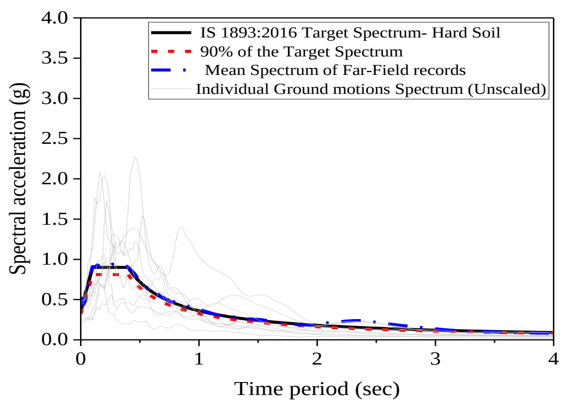

(b)

Figure 3 Scaled ground motions mean spectra and the target spectrum (a) near-field data, (b) far-field data

4. Results and Discussion

The subsequent sections delve into an examination of secondary structures' behavior. The acceleration time-history response of the secondary structure is studied in a few cases. The key response parameter used to characterize the performance of the secondary structure includes the Floor Response Spectrum (FRS).

4.1. Time History Response

The secondary structure's acceleration response is displayed in this section, as seen in Figure 4. The system depicted in Figure 1 is exposed to ground motions in order to study the impact of the dynamic interaction on the dynamic behavior of the SS. For this particular analysis, two ground motions (one near-field: RSN 802 and one far-field: RSN 1111) were selected from Table 1. These ground motions were chosen to have identical PGA and duration. The impact of the mass ratio (μ) and the SS damping ratio (ξ_s) on the SS's acceleration response is examined. The ratio of the mass of the secondary structure to the mass of the primary structure is known as the mass ratio (μ). For the coupled analysis, the values of μ are 0.001, 0.01, 0.1, and 0.5 are considered. For the purpose of this analysis, the PS (T_p) and SS (T_s) vibration periods are assumed to be 0.5 seconds. The SS (ξ_s) damping ratios are assumed to be 1% and 5%. As expected, the acceleration response's amplitude increases as the SS's damping ratio decreases. The seismic response of the secondary structure (SS) is not significantly affected by the dynamic interaction between the PS and SS when the mass ratio is as low as 0.001 (0.1%). This is evident as the acceleration response at μ = 0.001 closely resembles that of the uncoupled system. Therefore, at this mass ratio, the seismic demands on the secondary structure can be computed using the uncoupled analysis. The dynamic interaction between the PS and SS has a significant effect on the SS's acceleration response as the μ increases (μ = 1%, 10%, and 50%). A similar conclusion was observed in the study by (Kaiyuan *et al.,* 2023).

The peak acceleration response of the SS is shown in Table 2 for ξ_s = 5%, as peak values of any seismic response quantity provide important information about the bbehaviorof the structure. In comparison to the uncoupled evaluation conducted under NF and FF ground motions, Table 2 clearly demonstrates that for $\mu = 0.01$, 0.1, and 0.5, the peak acceleration response of the SS has decreased significantly. Under near-field (NF) excitation, the peak acceleration of the secondary structure (SS) experiences reductions of 15.7%, 68.3%, and 79.1% compared to the uncoupled case. Additionally, when compared to the uncoupled case, the peak acceleration of the secondary structure (SS) under far-field (FF) excitation decreases by 15.2%, 68.9%, and 78.8%. Overall, in both near- and far-field excitations, the secondary structure coupled with the primary structure shows notable reductions in peak accelerations compared to the uncoupled scenario. Furthermore, it is worth mentioning that near-field (NF) excitation tends to impose higher seismic demands on the secondary structure (SS), as evidenced by the data presented in Figure 4 and Table 2. In the specific scenario outlined in Table 2, it is observed that the response of the secondary structure (SS) exhibits an average increase of 10% under NF excitations compared to FF excitations. This finding underscores the notion that NF excitation imposes greater seismic loads on the SS (Bravo-Haro, Virreira and Elghazouli, 2021; Zhai *et al.,* 2016) in contrast to FF excitation. This trend highlights the importance of considering the specific characteristics of ground motion in assessing seismic performance. A similar pattern was seen for the ξ_s = 1% also.

Table 2 Peak acceleration of the SS (g) for ξ_s = 5%

Ground motion	Uncoupled Analysis	Coupled Analysis			
		μ=0.001	μ=0.01	μ=0.1	μ=0.5
NF	4.58	4.61	3.86	1.45	0.96
FF	4.16	4.17	3.51	1.29	0.88

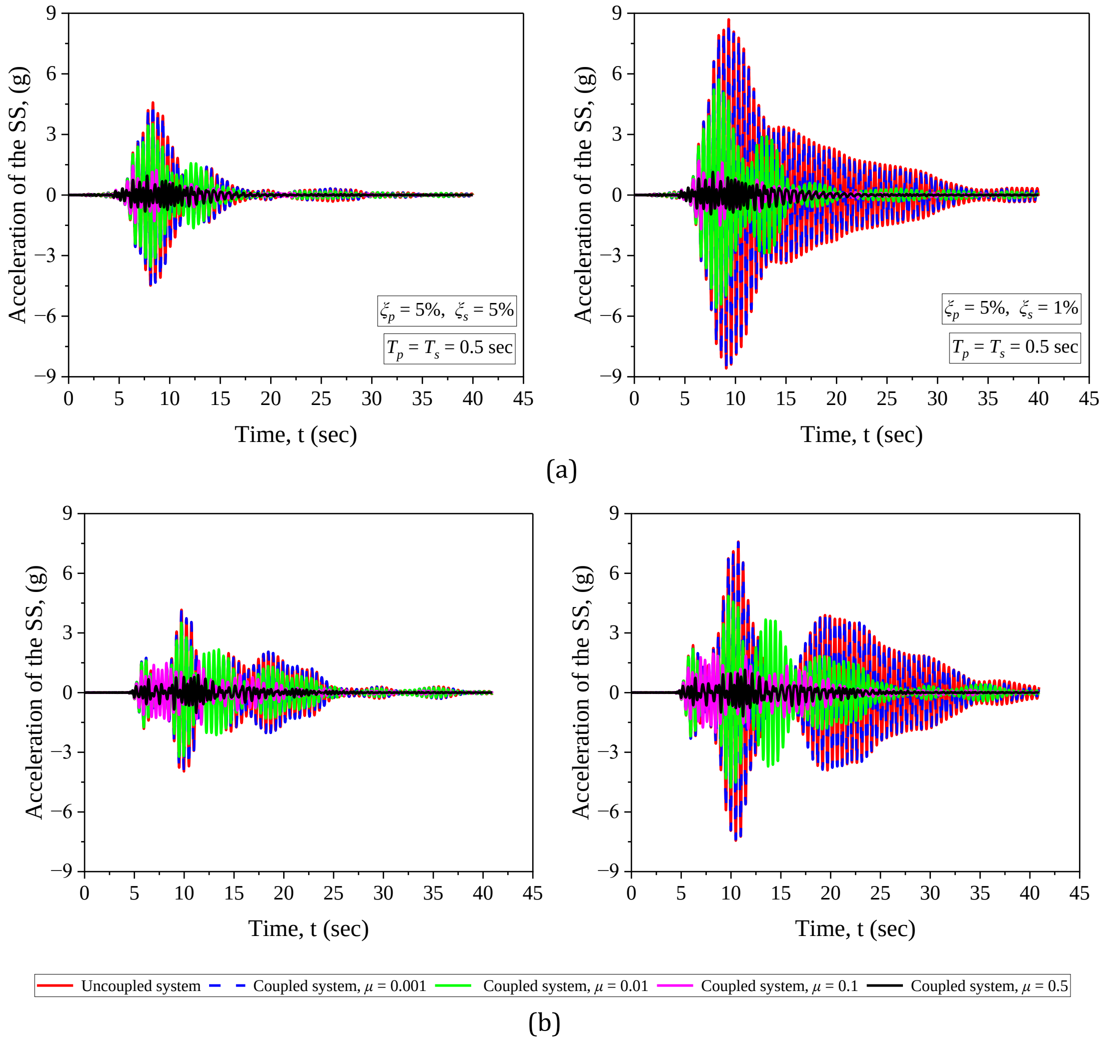

Figure 4 Time-history response (a) near-field data, (b) far-field data

4.2. Floor Response Spectrum

The maximum design forces for the design of the SS can be obtained from the floor response spectrum (FRS) approach (Haymes, Sullivan and Chandramohan, 2020). The FRS method disregards the PS and SS's dynamic interaction (Surana, Singh and Lang, 2018b; Adam, Furtmüller and Moschen, 2013). As a result, the current study tried to examine the FRS by considering the coupling effect. The floor response spectrum represents the SS's peak responses to input ground motion. The effects of the vibration period (T_p) of the PS, the mass ratio (μ), and the damping ratio (ξ_s) on the floor response spectrum are studied. For this purpose, scaled near- and far-field ground motions are input data for time history analyses. Absolute acceleration responses are individually obtained and subsequently utilized to calculate the corresponding FRS. These FRS are derived using a 5% damping ratio of the PS, and the mean results are then plotted and analyzed. The graphs depicted in Figures 5 and 6 illustrate the correlation between the average spectral acceleration (S_a, measured in g units) of an SS and the tuning ratio ($T_r = T_s/T_p$), where T_s is the vibration period of the SS. Analysis of Figures 5 and 6 reveals that dynamic interaction significantly influences the FRS within the range of $0.8 \leq T_r \leq 1.2$. Conversely, for $T_r < 0.5$ and $T_r > 2$, the impact of dynamic interaction appears negligible across all considered values of the damping ratio (ξ_s) and mass ratio (μ). Thus, it may be said that the coupling effect is noteworthy only when the T_s closely aligns with that of the PS, and a similar conclusion is observed in the study by (Zheng, Shi, and Sui, 2023). Regardless of the μ and type of ground motions, the S_a reduces with an increase in the primary structure's vibration period for a given damping ratio of the SS.

When the SS has lower damping ratios, there is a noticeable coupling impact on the FRS. These findings indicate that as the damping in the SS decreases, the dynamic interaction has a more significant impact on the FRS. Put differently, as the ξ_s decreases in the SS, the significance of the interaction in shaping the FRS becomes more pronounced. This observation underscores the importance of considering damping ratios, particularly in the SS, when analyzing the dynamic response of structures subjected to seismic forces. Peaks (in the vicinity of $0.8 \leq T_r \leq 1.2$) in the Floor Response Spectrum (FRS) show how the SS responds to earthquakes. When we look at these peaks at different mass ratios, we see that earthquakes nearby (near-field) make bigger peaks than those far away (far-field) at some combination of damping ratios and mass ratios.

As an illustration, consider the FRS value associated with the $T_r = 1$ to see the effect of near-field (NF) and far-field (FF) records on the seismic response of the SS. The analysis was conducted for different periods of vibration (T_p), including 0.1 sec, 0.5 sec, 1 sec, and 2 sec. For each T_p, the impact of NF and FF records on FRS was investigated across various ξ_s and μ. At T_p = 0.1 sec, it was observed that NF records consistently resulted in a decrease in S_a compared to FF records across all damping and mass ratios. The magnitude of these decreases varied, with higher damping ratios generally leading to larger percentage decreases.

At T_p = 0.5 sec, the influence of NF records on S_a exhibited variability depending on the damping and mass ratios. For μ = 0.01 and μ = 0.5, NF records consistently yielded higher S_a values, indicating a significant effect. However, for μ = 0.1, NF records showed a slight decrease in Sa compared to FF records, suggesting a less pronounced impact. At T_p = 1 sec, similar variability in the influence of NF records on S_a was observed. For μ = 0.01 and μ = 0.1, NF records consistently led to lower S_a values, indicating a significant effect. Conversely, for μ = 0.5, NF records showed a slight increase in S_a compared to FF records. Finally, at T_p = 2 sec, the pattern of influence of NF records on S_a varied based on the damping and mass ratios. NF records consistently resulted in higher S_a values for μ = 0.01 and μ = 0.5, indicating a significant effect. However, for μ = 0.1, NF records showed a slight decrease in S_a compared to FF records, suggesting a less pronounced impact. These findings underscore the complex interplay between ground motion characteristics, ξ_s, and the μ in influencing secondary structural response to seismic events.

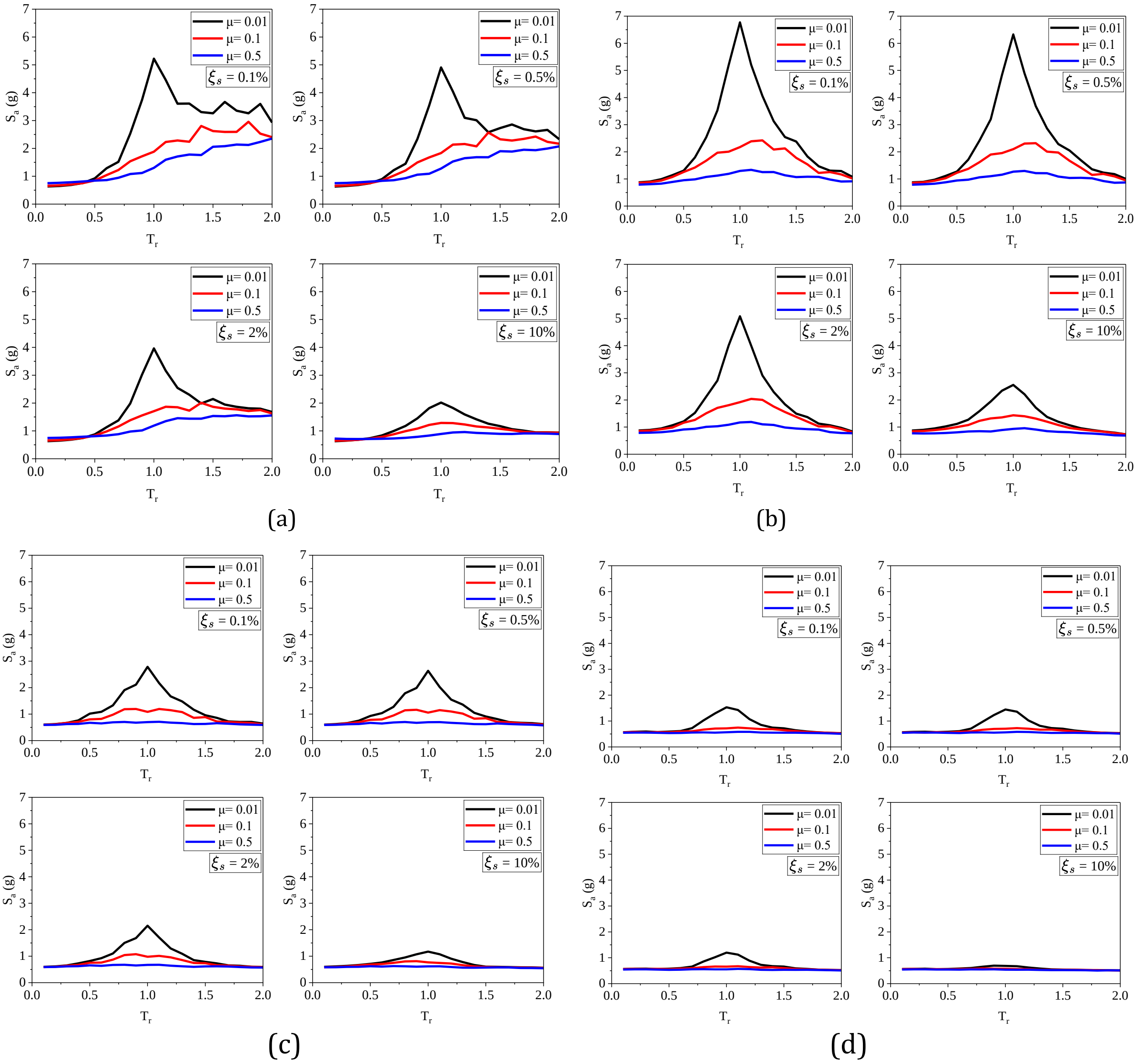

Figure 5 FRS Vs. tuning ratio under near-field records for (a) T_p = 0.1 sec, (b) T_p = 0.5 sec, (c) T_p = 1 sec, (d) T_p = 2 sec

The vibration period of the primary structure is a critical factor in determining its response to ground motion. Structures with shorter periods are more susceptible to the high-frequency motions characteristic of near-field (NF) records, whereas longer-period structures are predominantly influenced by the lower-frequency content typical of far-field (FF) records. It is essential to emphasize the significance of considering both NF and FF records in seismic hazard assessment and structural design. From Sections 4.1 and 4.2, the important points or analysis results can be summarized as follows:

- The dynamic interaction between the primary structure (PS) and secondary structure (SS) significantly affects the acceleration response of the SS, particularly when the mass ratio (μ) is high. For low mass ratios (μ = 0.001), the acceleration response of the SS is similar to that of the uncoupled system, indicating minimal impact of dynamic interaction.
- Near-field (NF) ground motions tend to impose higher seismic demands on the SS compared to far-field (FF) ground motions.

- Lower damping ratios in the SS result in a more pronounced coupling impact on the FRS. This emphasizes the importance of considering the damping ratio of the SS when analyzing the dynamic response of structures subjected to seismic forces.
- At certain vibration periods and mass ratios, NF records unexpectedly result in lower spectral accelerations (S_a) compared to FF records, which is contrary to the general trend observed. This suggests that NF ground motions do not always impose higher seismic demands, highlighting the complexity of seismic response behavior.
- The significant reduction in peak accelerations for SS coupled with PS under NF and FF excitations is noteworthy. This indicates that coupled systems may perform better in terms of seismic demands compared to uncoupled systems, challenging the conventional assumption that coupling always increases seismic demands.
- The finding that lower damping ratios in SS enhance the impact of dynamic interaction on FRS was unexpected. This underscores the need for detailed consideration of damping properties in seismic analysis and design, as it significantly affects the seismic response of SS.

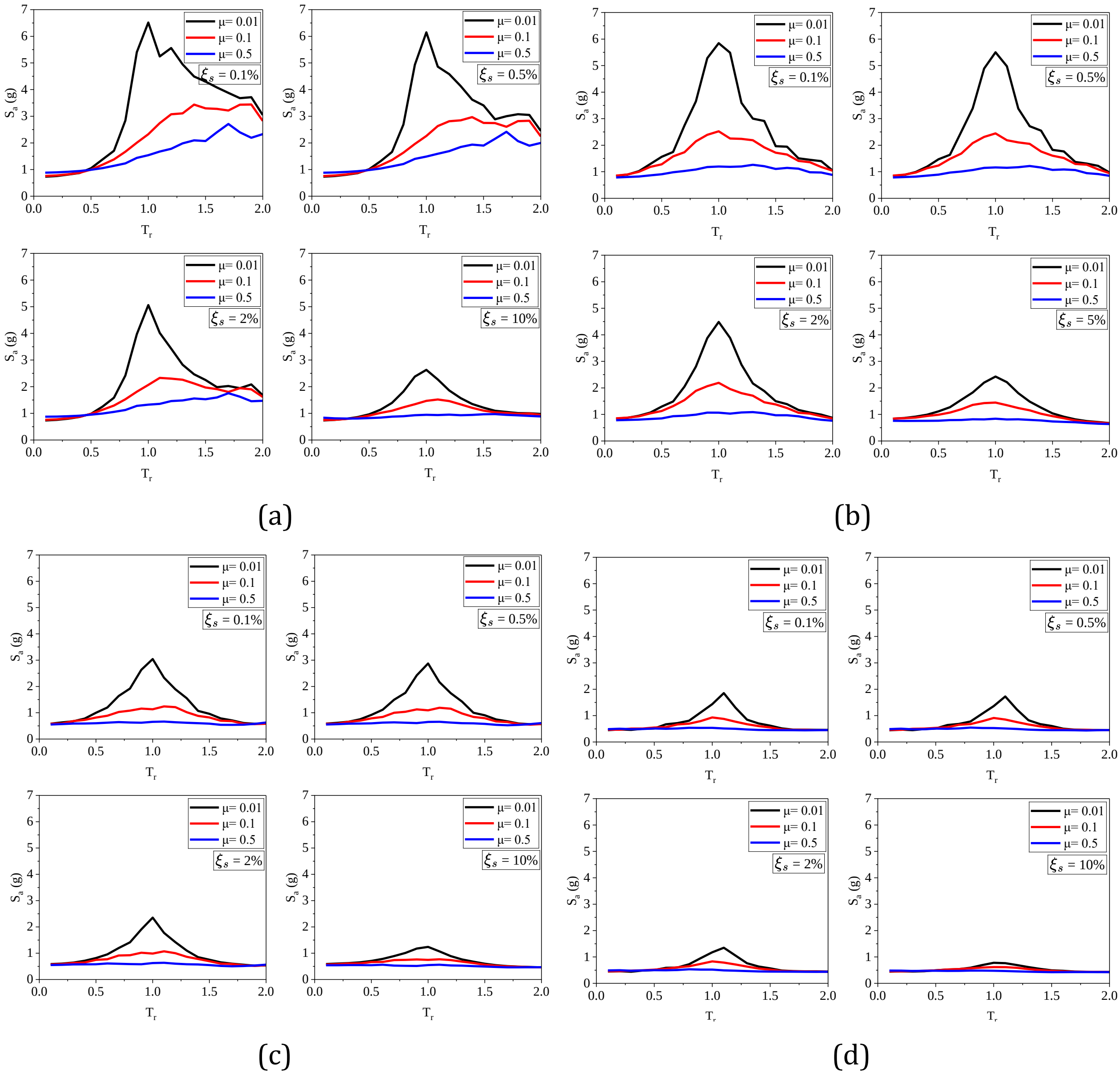

Figure 6 FRS Vs. tuning ratio under far-field records for (a) T_p = 0.1 sec, (b) T_p = 0.5 sec, (c) T_p = 1 sec, (d) T_p = 2 sec

The findings underscore the need for site-specific analyses that account for the complex interplay between ground motion characteristics and structural response. This conclusion underscores the importance of considering the source-to-site distance and the ground motion characteristics when assessing the seismic response of PS and SS to withstand earthquakes.

4.3. Comparing the FRS with Eurocode 8 (EC8) Formula

A comparative examination between the FRS generated in this study using near-field (NF) and far-field (FF) records and the approach outlined in Eurocode 8 (NSAI, 2005) is conducted in the present section. Eurocode 8 provides a formulation for computing the spectral acceleration (S_a) applied to a SS, as depicted in Equation 11:

$$S_a = \alpha . S . \left[\frac{3.\ (1 + z/H)}{1 + (1 - T_s/T_p)^2} - 0.5 \right] . g \geq \alpha . S . g \tag{11}$$

where α represents the ratio of ground acceleration to gravity g, while S denotes a soil amplification factor. The term z/H indicates the relative height of the structure where the component is located, T_s stands for the period of the secondary structure and T_p represents the primary structure's vibration period.

Two fundamental factors affect the design of FRS: the tuning ratio (T_r) and the relative height of the SS. The formula provided by Eurocode provides a series of curves that show the highest spectral acceleration values for each floor when T_s equals T_p. Plots of the elastic generated and the Eurocode 8 (EC8) spectra are shown for the PS under consideration in Figure 7 and 8.

When the mass of SS is negligible (μ = 0.01), the EC8 approach tends to underestimate the maximum demand for SSs at $0.8 \leq T_r \leq 1.2$ under both near-field (NF) and far-field (FF) seismic records, assuming a primary structure with T_p = 0.5 sec and varying ξ_s. For T_p = 1 sec, under NF and FF records, the EC8 formulation underestimates the maximum demand for SSs with damping ratios of ξ_s = 0.1% and 0.5%. Conversely, for damping ratios of ξ_s = 2% and 10%, the EC8 tends to overestimate the maximum demand for SSs. In contrast, for SSs with mass ratios, μ = 0.1 & 0.5, in both near-field (NF) and far-field (FF) records, the EC8 formulation tends to predict higher floor acceleration demands across various ξ_s of the SS within the same T_r range. If T_r falls below 0.5, the EC8 consistently predicts higher demands on SSs without regard to mass ratios, damping ratios, primary structure type, or record type. Conversely, when T_r surpasses 2.5, the EC8 consistently underestimates demands on SSs, regardless of mass ratios and damping ratios for a flexible primary structure (T_p = 1 sec). The dynamic interaction between the primary and secondary structures is thus not considered by the EC8 formulation. Figure 7 and 8 show a notable discrepancy in which the floor spectral acceleration is either greatly overestimated or underestimated by the criteria given in EC8. This inconsistency emphasizes the requirement of updating the code-based approach. To enhance the accuracy of the formulation, it is crucial to incorporate the effects of dynamic interaction between the PS and SS. This adjustment is vital for improving the seismic evaluation of secondary structures, as it aligns code-based predictions more closely with observed spectrum accelerations.

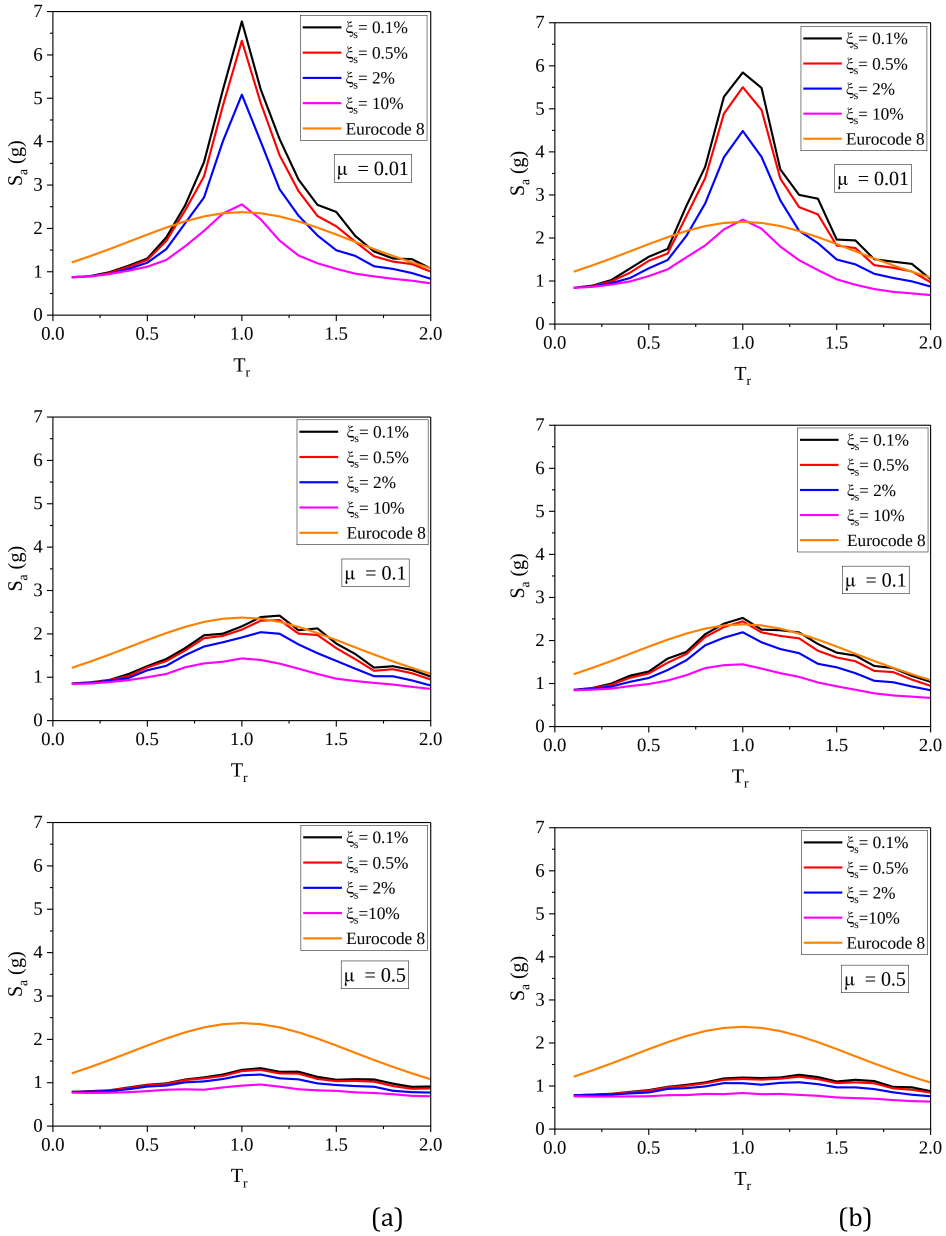

Figure 7 Comparing the predicted FRS of a PS (T_p = 0.5 sec) with code-based FRS for (a) near-field records and (b) far-field records

4.4. Engineering Application

The above analysis results can be effectively utilized in practical engineering applications, such as the seismic design of hospital equipment. Hospitals house numerous critical secondary structures (SS), such as medical equipment, electrical panels, and storage units, which are essential for patient care and hospital operations. Ensuring the functionality of these structures during and after an earthquake is crucial. The dynamic interaction between the hospital building (PS) and these secondary structures can significantly impact their seismic response. The present research findings can be applied in the practical field as follows:

- Hospital equipment can be modeled as single-degree-of-freedom (SDOF) systems, characterized by parameters such as mass ratio (μ), damping ratio (ξ_s), and vibration period (T_s). This modeling allows for a detailed understanding of the equipment's behavior during seismic events.

- Ground motion records, including both near-field (NF) and far-field (FF) events, can be used to simulate the seismic response of the hospital building and its equipment. Numerical tools like MATLAB can facilitate these simulations, providing realistic scenarios of seismic activity.
- The research shows how the peak acceleration response of secondary structures varies with different mass and damping ratios. These insights help in predicting the seismic demands on the equipment.
- Understanding that dynamic interaction is minimal at very low mass ratios ($\mu = 0.001$) and significant at higher mass ratios allows engineers to optimize the design of equipment supports and anchors. Robust anchoring systems can be designed for equipment with higher mass ratios to ensure they can withstand seismic forces effectively.
- The study's findings on the Floor Response Spectrum (FRS) can be applied to derive maximum design forces for hospital equipment. By considering the coupling effects, the FRS method provides a more accurate estimate of seismic demands, preventing over- or under-design.

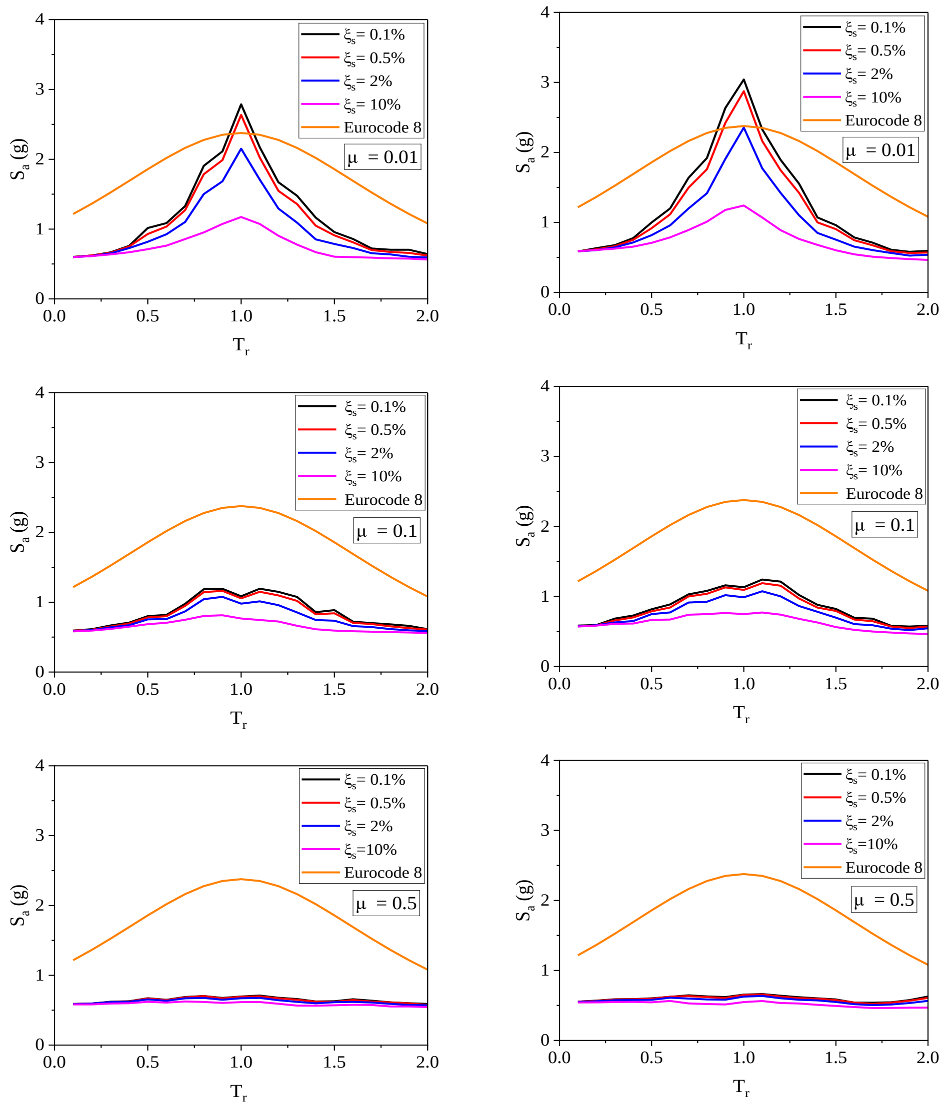

(a) (b)

Figure 8 Comparing the predicted FRS of a PS (T_p = 1 sec) with code-based FRS for (a) near-field records and (b) far-field records

5. Conclusions

The purpose of this article is to examine how dynamic interaction affects secondary structures' seismic needs. This paper delves into a parametric investigation of the dynamic interaction between primary and secondary structures. The dynamic interaction exhibits a notable impact on the acceleration demands of the SS with increasing mass ratio. Near-Field excitations impose greater seismic loads on the SS in contrast to Far-Field excitations. At a very low mass ratio (μ = 0.001), the dynamic interaction is negligible. For μ values of 0.01, 0.1, and 0.5, the peak acceleration response of the SS under near-field (NF) excitation decreased by 15.7%, 68.3%, and 79.1%, respectively, and by 15.2%, 68.9%, and 78.8% under far-field (FF) excitation, compared to the uncoupled case. Only in the cases when the secondary structure closely matches the main structure's vibration period—that is, in the region of $0.8 \leq T_r \leq 1.2$—is coupled analysis required. Conversely, for $T_r < 0.5$ and $T_r > 2$, the influence of interaction on the FRS appears insignificant across all examined values of ξ_s and μ.

Lower damping ratios (ξ_s) in the SS increase the significance of dynamic interaction on the FRS. Peaks in the FRS within the range of $0.8 \leq T_r \leq 1.2$ show higher responses to NF excitations compared to FF excitations. The finding that lower damping ratios in SS enhance the impact of dynamic interaction on FRS was unexpected. This underscores the need for detailed consideration of damping properties in seismic analysis and design, as it significantly affects the seismic response of SS. The Floor Response Spectrum (FRS) provides essential insights into the seismic response of secondary structures (SSs), particularly within the range of 0.8 ≤ T_r ≤ 1.2, where peaks are most prominent. Near-field (NF) earthquakes tend to generate larger peaks in FRS compared to far-field (FF) events, especially at specific combinations of damping and mass ratios. Our analysis across various vibration periods (T_p) highlights the nuanced impact of NF and FF records on spectral accelerations (S_a). Notably, NF records consistently lead to higher S_a values for shorter periods (T_p = 0.1 sec), while the influence varies at longer periods.

The design of FRS is influenced by the relationship between the period of secondary structure (SS) and the primary structural system. However, the current Eurocode 8 (EC8) formulation doesn't fully account for this dynamic interaction. Our analysis found that for lightweight SS (μ = 0.01), EC8 underestimates maximum floor acceleration demands in certain scenarios, while for heavier SS (μ = 0.1 & 0.5), it tends to overestimate them. Additionally, EC8 consistently overestimates acceleration demands when $T_r < 0.5$ and underestimates them when $T_r > 2$. This discrepancy highlights the need to revise EC8 to consider the effects of dynamic interaction. Incorporating these effects will improve the accuracy of predictions and ensure better seismic performance of secondary structures.

Acknowledgments

The authors would like to acknowledge the support of Prince Sultan University in paying the Article Processing Charges (APC) for this publication.

References

Adam, C., Furtmüller, T., Moschen, L., 2013. Floor Response Spectra For Moderately Heavy Nonstructural Elements Attached To Ductile Frame Structures. In: *Computational Methods in Earthquake Engineering*. Volume 2, pp. 69–89

Akbari, J., Rozbahani, S., Isari, M., 2021. Effect of Moving Resonance on The Seismic Responses Under Far-Field and Near-Field Earthquakes. *Asian Journal of Civil Engineering*, Volume 22, pp. 159–173

American Society of Civil Engineers (ASCE), 2016. Minimum Design Loads and Associated Criteria for Buildings and Other Structures. *American Society of Civil Engineers,* pp. 7–16

Annamdasu, M.L., Challagulla, S.P., Kontoni, D.-P.N., Rex, J., Jameel, M., Vicencio, F., 2024. Artificial Neural Network-Based Prediction Model of Elastic Floor Response Spectra Incorporating Dynamic Primary-Secondary Structure Interaction. *Soil Dynamics and Earthquake Engineering*, Volume 177, p. 108427

Berto, L., Bovo, M., Rocca, I., Saetta, A., Savoia, M., 2020. Seismic Safety of Valuable Non-Structural Elements in RC Buildings: Floor Response Spectrum Approaches. *Engineering Structures*, Volume 205, p. 110081

Bhavani, B.D., Challagulla, S.P., Noroozinejad Farsangi, E., Hossain, I. and Manne, M., 2023. Enhancing Seismic Design of Non-structural Components Implementing Artificial Intelligence Approach: Predicting Component Dynamic Amplification Factors. *International Journal of Engineering*, Volume 36(7), pp. 1211–1218

Bravo-Haro, M.A., Virreira, J.R., Elghazouli, A.Y., 2021. Inelastic Displacement Ratios for Non-Structural Components In Steel Framed Structures Under Forward-Directivity Near-Fault Strong-Ground Motion. *Bulletin of Earthquake Engineering*, Volume 19, pp. 2185–2211

Challagulla, S.P., Bhavani, B.D., Suluguru, A.K., Jameel, M., Vicencio, F., 2023a. Influence of Ground Motion Scaling on Floor Response Spectra. *Current Science*, Volume 124(8), p. 928

Challagulla, S.P., Kontoni, D.-P.N., Suluguru, A.K., Hossain, I., Ramakrishna, U., Jameel, M., 2023b. Assessing the Seismic Demands on Non-Structural Components Attached to Reinforced Concrete Frames. *Applied Sciences*, Volume 13(3), p. 1817

Challagulla, S.P., Parimi, C., Anmala, J., 2020. Prediction of Spectral Acceleration of A Light Structure with a Flexible Secondary System Using Artificial Neural Networks. *International Journal of Structural Engineering*, Volume 10(4), pp. 353–379

Challagulla, S.P., Parimi, C., Noroozinejad Farsangi, E., 2022. Effect of Flexibly Attached Secondary Systems on Dynamic Behavior of Light Structures. *Practice Periodical on Structural Design and Construction*, Volume 27(1), p. 4021057

Challagulla, S.P., Parimi, C., Thiruvikraman, P.K., 2020. Effect of the Sliding of Stacked Live Loads on the Seismic Response of Structures. *Engineering Journal*, Volume 24(4), pp. 97–110

Faisal, A., Anshari, A., Nazri, F.M., Kassem, M.M., 2023. Near-Collapse Probability of RC Frames in Indonesia Under Repeated Earthquakes Containing Fling-Step Effect. *International Journal of Technology,* Volume 14(2), pp. 339–350

Federal Emergency Managemnt Agency (FEMA), 2009. *Quantification of Building Seismic Performance Factors*. US Department of Homeland Security, Federal Emergency Managemnt Agency (FEMA)

Filiatrault, A., Perrone, D., Merino, R.J., Calvi, G.M., 2018. Performance-Based Seismic Design of Nonstructural Building Elements. *Journal of Earthquake Engineering*, Volume 25(2), pp. 237–269

Haymes, K., Sullivan, T.J., Chandramohan, R., 2020. A Practice-Oriented Method for Estimating Elastic Floor Response Spectra. *Bulletin of the New Zealand Society for Earthquake Engineering*, Volume 53(3), pp. 116–136

Igusa, T., Der-Kiureghian, A., 1985. Dynamic Characterization of Two-Degree-of-Freedom Equipment-Structure Systems. *Journal of Engineering Mechanics*, Volume 111(1), pp. 1–19

Indian Standard, 2016. Industrial Structures Including Stack-Like Structures. *In: Criteria For*

Earthquake Resistant Design of Structures. IS 1893, 2016
Kaiyuan, Z., Xudong, Z., Feng, F., Peng, D., Jun, G., 2023. Experimental And Numerical Studies of The Dynamic Coupling Effect In The Primary-Secondary System. *Structures*, Volume 54, pp. 732–745
Kamble, V., Bharti, S.D., Shrimali, M.K., 2021. Seismic Response of the Secondary Piping System under Bi-Directional Earthquake. *Asian Journal of Civil Engineering*, Volume 22(6), pp. 1221–1234
Kamble, V., Dayal Bharti, S., Kumar Shrimali, M., Kanti Datta, T., 2022. Control of Secondary Systems Response in a Base-Isolated Building under Tridirectional Ground Motion. *Practice Periodical on Structural Design and Construction*, Volume 27(1), p. 04021060
Kelly, J.M., Sackman, J.L., 1978. Response Spectra Design Methods For Tuned Equipment-Structure Systems. *Journal of Sound and Vibration*, Volume 59(2), pp. 171–179
Landge, M.V., Ingle, R.K., 2021. Comparative Study of Floor Response Spectra for Regular and Irregular Buildings Subjected to Earthquake. *Asian Journal of Civil Engineering*, Volume 22(1), pp. 49–58
Lim, E., Chouw, N., 2018. Prediction of the Response of Secondary Structures Under Dynamic Loading Considering Primary–Secondary Structure Interaction. *Advances in Structural Engineering*, Volume 21(14), pp. 2143–2153
Lin, J., 2022. Vibration Reduction Performance of Structures with Viscous Dampers under Near-Field Earthquakes. *Advances in Civil Engineering*, Volume 2022(1), p. 1315213
Mehta, R., Bhandari, M., 2023. Evaluation of Seismic Response of Composite Buildings under Near-Field Earthquakes. *In:* IOP Conference Series: Earth and Environmental Science. IOP Publishing. p. 12016
Murty, C.V.R., Goswami, R., Vijayanarayanan, A.R., Kumar, R.P., Mehta, V.V., 2012. Earthquake Protection of Non-Structural Elements in Buildings. *Gujarat State Disaster Management Authority*, Volume 2012, pp. 1–145
National Standards Authority of Ireland (NSAI), 2005. Eurocode 8: Design of Structures for Earthquake Resistance-Part 1: General Rules, Seismic Actions and Rules For Buildings. I.S. EN 1998-1:2005. European Committee for Standardization, Brussels
Partono, W., Irsyam, M., Nazir, R., Asrurifak, M., Sari, U.C., 2022. Site Coefficient and Design Spectral Acceleration Evaluation of New Indonesian 2019 Website Response Spectra. *International Journal of Technology,* Volume 13(1), pp. 115–124
Pesaralanka, V., Challagulla, S.P., Vicencio, F., Chandra Babu, P.S., Hossain, I., Jameel, M., Ramakrishna, U., 2023. Influence of a Soft Story on the Seismic Response of Non-Structural Components. *Sustainability*, Volume 15(4), p. 2860
Pramono, S., Prakoso, W.A., Rohadi, S., Karnawati, D., Permana, D., Prayitno, B.S., Rudyanto, A., Sadly, M., Sakti, A.P., Octantyo, A.P., 2020. Investigation of Ground Motion and Local Site Characteristics of the 2018 Lombok Earthquake Sequence. *International Journal of Technology,* Volume 11(4), pp. 743–753
Reyes, J.C., Ardila-Bothia, L., Smith-Pardo, J.P., Villamizar-Gonzalez, J.N., Ardila-Giraldo, O.A., 2016. Evaluation of The Effect of Containers on The Seismic Response of Pile-Supported Storage Structures. *Engineering Structures*, Volume 122, pp. 267–278
Reyes, J.C., Herrera, M.T., Smith-pardo, J.P., Córdoba, L.S., 2020. Effective Live Load Mass for Storage Buildings on Friction-Pendulum Isolators. *Engineering Structures,* Volume 218, p. 110843
Sackman, J.L., Kelly, J.M., 1979. Seismic Analysis of Internal Equipment and Components in Structures. *Engineering Structures*, Volume 1(4), pp. 179–190
Salimbahrami, S.R., Gholhaki, M., 2022. Response of Concrete Buildings with Steel Shear Walls to Near-and Far-Field Earthquakes. *In:* Proceedings of the Institution of Civil

Engineers-Structures and Buildings, Volume 175(1), pp. 17–33

Salman, K., Tran, T.T., Kim, D., 2019. Grouping Effect on The Seismic Response of Cabinet Facility Considering Primary-Secondary Structure Interaction. *Nuclear Engineering and Technology*, Volume 52(6), pp. 1318–1326

Singh, M.P., Suarez, L.E., 1987. Seismic Response Analysis of Structure–Equipment Systems with Non‐Classical Damping Effects. *Earthquake Engineering & Structural Dynamics*, Volume 15(7), pp. 871–888

Smith-Pardo, J.P., Reyes, J.C., Ardila-Bothia, L., Villamizar-Gonzalez, J.N., Ardila-Giraldo, O.A., 2015. Effect of Live Load on The Seismic Design of Single-Story Storage Structures Under Unidirectional Horizontal Ground Motions. *Engineering Structures*, Volume 93, pp. 50–60

Suarez, L.E., Singh, M.P., 1987. Floor Response Spectra with Structure–Equipment Interaction Effects by a Mode Synthesis Approach. *Earthquake Engineering & Structural Dynamics*, Volume 15(2), pp. 141–158

Sullivan, T.J., 2020. Post-Earthquake Reparability of Buildings: The Role of Non-Structural Elements. *Structural Engineering International*, Volume 30(2), pp. 217–223

Surana, M., Singh, Y., Lang, D.H., 2018a. Effect of Irregular Structural Configuration On Floor Acceleration Demand In Hill-Side Buildings. *Earthquake Engineering and Structural Dynamics*, Volume 47(10), pp. 2032–2054

Surana, M., Singh, Y., Lang, D.H., 2018b. Floor Spectra of Inelastic RC Frame Buildings Considering Ground Motion Characteristics. *Journal of Earthquake Engineering*, Volume 22(3), pp. 488–519

Taghavi, S., Miranda, E., 2004. Estimation of Seismic Acceleration Demands in Building Components. *In:* 13th World Conference on Earthquake Engineering Vancouver, p. 3199

Villaverde, R., 2009. *Fundamental Concepts of Earthquake Engineering*. CRC Press

Vyshnavi, P., Challagulla, S.P., Adamu, M., Vicencio, F., Jameel, M., Ibrahim, Y.E., Ahmed, O.S., 2023. Utilizing Artificial Neural Networks and Random Forests to Forecast the Dynamic Amplification Factors of Non-Structural Components. *Applied Sciences*, Volume 13(20), p. 11329

Wang, T., Shang, Q., Li, J., 2021. Seismic Force Demands on Acceleration-Sensitive Nonstructural Components: a State-Of-The-Art Review. *Earthquake Engineering and Engineering Vibration*, Volume 20(1), pp. 39–62

Yaakub, A.R., Evans, D.J., 1999. A fourth order Runge–Kutta RK(4,4) Method With Error Control. *International Journal of Computer Mathematics*, Volume 71(3), pp. 383–411

Zamanian, M., Kheyroddin, A., Mortezaei, A., 2022. Study on Passive and Semiactive Control Systems in Structures under Near-and Far-Field Earthquakes. *Shock and Vibration*, Volume 2022(1), p. 1103434

Zhai, C.H., Zheng, Z., Li, S., Pan, X., Xie, L.L., 2016. Seismic Response Of Nonstructural Components Considering The Near-Fault Pulse-Like Ground Motions. *Earthquake and Structures*, Volume 10(5), pp. 1213–1232

Zheng, Z., Shi, C., Sui, X., 2023. Sensitivity Study of Coupling Effect of Upper Substructure on Main Structure in Floor Response Spectrum Analysis of Nuclear Power Plant Building. *In:* International Conference on Advanced Civil Engineering and Smart Structures. pp. 58–67